

# Are the $J/\psi$ and $\chi_c$ $A$ Dependencies the Same?

R. Vogt<sup>1</sup>

*Niels Bohr Institute, Blegdamsvej 17, DK-2100 Copenhagen  
Nuclear Science Division, Lawrence Berkeley National Laboratory, Berkeley, CA  
94720, USA*

*Physics Department, University of California at Davis, Davis, CA 95616, USA*

## Abstract

It has been empirically observed that the dependence of  $J/\psi$  and  $\psi'$  production on nuclear mass number  $A$  is very similar. This has been postulated to be due to the predominance of color octet pre-resonant states in charmonium production and absorption. Two new experiments, NA60 at CERN and HERA-B at DESY, will measure the  $\chi_c$   $A$  dependence for the first time. These measurements should shed new light on the charmonium production and absorption mechanisms.

PACS: 24.85.+p, 25.40.Ep

---

<sup>1</sup>This work was supported in part by the Director, Office of Energy Research, Division of Nuclear Physics of the Office of High Energy and Nuclear Physics of the U. S. Department of Energy under Contract Number DE-AC03-76SF00098.

# 1 Introduction

The description of particle production in proton-nucleus interactions as a simple scaling of the proton-proton production cross section with nuclear mass number  $A$ ,

$$\sigma_{pA} = \sigma_{pN} A^\alpha, \quad (1)$$

has been used to describe many processes. When the production of the desired final state particle is calculable in perturbative QCD, the factorization theorem [1] suggests that the exponent  $\alpha$  should be unity. Drell-Yan production, integrated over all kinematic variables, agrees with  $\alpha = 1$  to rather high precision [2] although some deviation from unity appears at large values of Feynman  $x$ ,  $x_F = p_{\parallel}/p_{\max}$ . A less than linear  $A$  dependence has been observed for  $J/\psi$ ,  $\psi'$ ,  $\Upsilon$ , and  $\Upsilon' + \Upsilon''$  production with  $0.9 < \alpha < 1$  near  $x_F \approx 0$ .

By now, the  $A$  dependence of  $J/\psi$  production at  $x_F > 0$  is known to rather high precision at several different energies [3, 4, 5, 6, 7, 8]. While the  $\psi'$   $A$  dependence is not as accurately known, its statistics were sufficient for the E866 collaboration to determine that the  $\psi'$   $\alpha$  is smaller than the  $J/\psi$   $\alpha$  for  $x_F < 0.2$  [8]. The known  $A$  dependence of  $J/\psi$  production has been used to determine the strength of the “anomalous”  $J/\psi$  suppression in Pb+Pb interactions at the CERN SPS [9]. However, an important assumption in this interpretation is that all charmonium states interact with the nucleus while in “pre-resonant”  $|(c\bar{c})_{8g}\rangle$  states [10]. Since a significant fraction,  $\sim 40\%$ , of the observed  $J/\psi$ 's come from  $\chi_c$  decays [11, 12, 13, 14, 15, 16, 17, 18, 19, 20, 21], a measurement of the  $\chi_c$   $A$  dependence is crucial for the understanding of  $J/\psi$  suppression in nucleus-nucleus collisions because in a quark-gluon plasma,  $J/\psi$  suppression is expected to occur in steps, the first of which is the dissociation of the  $\chi_c$  [22]. So far, only one experiment [20] has presented differential distributions of  $\chi_c$  production, albeit with such a small sample that it is not possible to tell if the shapes of the  $\chi_c$  and  $J/\psi$   $x_F$  distributions are the same or not. No measurement of the  $\chi_c$   $A$  dependence has yet been made.

Fortunately, this situation seems about to change. The  $\chi_c$   $A$  dependence will be measured for the first time in two fixed-target experiments at different energies. The NA60 collaboration, a follow-up to the NA50 collaboration at CERN, has been approved for  $pA$  measurements at 450 GeV and is planning to also take data in nucleus-nucleus interactions at 158 GeV [23, 24]. Their muon spectrometer will sit at  $0 < y_{\text{cm}} < 1$  at both energies, giving forward  $x_F$  coverage only. The HERA-B collaboration at DESY has placed target wires around the halo of the proton beam at HERA. In their first run, they have demonstrated that they can detect the  $\chi_c$  [25, 26]. In their next run, they will measure the  $J/\psi$ ,  $\psi'$ , and  $\chi_c$   $A$  dependence over  $-0.5 < x_F < 0.3$ . This will thus be the first charmonium experiment with coverage significantly below  $x_F \sim -0.1$ .

If the  $A$  dependence of  $\chi_c$  production is the same as that of the  $J/\psi$ , then the picture of a pre-resonant color octet state passing through the target [10] will be validated. Then charmonium production and absorption at fixed-target energies can be essentially described within the color evaporation model [27]. However, the non-relativistic QCD model [28, 29] predicts that  $\chi_c$  production should be predominantly

color singlet while direct  $J/\psi$  and  $\psi'$  production is via color octet states. If this picture is correct, the  $A$  dependence of  $\chi_c$  production could be quantitatively different than that of the  $J/\psi$  and  $\psi'$ .

In this paper we focus only on charmonium production and its subsequent absorption by nucleons, the “normal absorption” identified by NA50 [9]. While this is insufficient to describe  $\alpha(x_F)$  over the full range of  $x_F$ , the NA60 and HERA-B measurements will be in a region where the  $x_F$  dependence of  $\alpha$  has so far either not been determined or has not been strong [8]. At larger negative  $x_F$ , the  $A$  dependence may be different than expected from pre-resonant absorption [10]. Other nuclear effects such as shadowing, energy loss, and intrinsic heavy quarks depend only on either the projectile or target momentum fractions and not on the identity of the final charmonium state [30] and thus should affect  $J/\psi$  and  $\chi_c$  production identically. We first discuss charmonium production by color evaporation and nonrelativistic QCD and then describe how nuclear absorption of color octet and color singlet states might be disentangled.

## 2 Charmonium Production: Color Evaporation vs. NRQCD

Two models have been used to describe quarkonium hadroproduction: the color evaporation model (CEM) and the nonrelativistic QCD model (NRQCD). Since both have been described in detail elsewhere, we only discuss the specifics that are germane to our calculation.

In the CEM, charmonium production is a subset of the  $c\bar{c}$  pairs produced below the  $D\bar{D}$  threshold. The hadronization of charmonium state  $C$  from these sub-threshold  $c\bar{c}$  pairs is accomplished through the emission of one or more soft gluons. It is assumed that the hadronization does not affect the kinematics of the parent  $c\bar{c}$  pair so that only a single universal factor,  $F_C$ , is necessary for each state. The factor  $F_C$  depends on the charm quark mass,  $m_c$ , the scale  $\mu$  of the strong coupling constant  $\alpha_s$ , and the parton densities. We use the MRST LO parton distributions [31, 32] for CEM production. The factor  $F_C$  must be constant for the model to have any predictive power. The differential and integrated quarkonium production rates should thus be proportional to each other and independent of projectile, target, and energy. The relative charmonium rates so far seem to bear this out since  $\sum_J \chi_{cJ}/(J/\psi) \approx 0.4$  and  $\psi'/(J/\psi) \approx 0.14$  [18, 19, 21, 33, 34] over a wide range of targets and energies, see also Ref. [27].

The LO cross section of state  $C$ ,  $\tilde{\sigma}_C$ , from projectile  $p$  and target  $A$  is

$$\begin{aligned} \frac{d\tilde{\sigma}_C}{dx_F} &= 2F_C^{\text{NLO}} K \int_{2m_c}^{2m_D} m dm \int_0^1 dx_1 dx_2 \delta(x_1 x_2 s - m^2) \delta(x_F - x_1 + x_2) \\ &\times \left\{ f_g^p(x_1, m^2) f_g^A(x_2, m^2) \sigma_{gg}(m^2) \right. \\ &\left. + \sum_{q=u,d,s} [f_q^p(x_1, m^2) f_q^A(x_2, m^2) + f_q^p(x_1, m^2) f_q^A(x_2, m^2)] \sigma_{q\bar{q}}(m^2) \right\}. \quad (2) \end{aligned}$$

The partonic cross sections  $\sigma_{gg}$  and  $\sigma_{q\bar{q}}$  can be found in Ref. [35, 36]. Production by quark-gluon scattering enters only at NLO.

A  $K$  factor was included in Eq. (2) since our calculation is at leading order and  $F_C$  was determined at next-to-leading order, as indicated. At NLO, the charmonium cross section was calculated using the  $Q\bar{Q}$  production code of Ref. [37] with a cut on the pair mass as in Eq. (2) [27]. The  $p_T$  dependence and the normalization of the charmonium cross section from the Tevatron collider agrees with these calculations [38]. Since, at fixed energy, the  $K$  factor for  $c\bar{c}$  production is independent of the kinematic variables [39], our calculation is at leading order. Therefore, we multiply the LO cross section by  $K$  to obtain the magnitude of the NLO cross section and then also by  $F_C^{\text{NLO}}$  to fix the hadronization of the subthreshold  $c\bar{c}$  pairs to charmonium. Note however that since we study ratios of cross sections, only the relative normalization is important and because no nuclear effects on the parton densities are included, the CEM production information generally cancels.

Since the CEM depends on the universality of charmonium hadronization through soft gluon emission, a check of this assumption for  $\chi_c$  production, particularly as a function of  $x_F$ , is critical. The  $\chi_c$  has previously been crucial for furthering the understanding of charmonium production. The color singlet model (CSM) [40, 41] described high  $p_T$  charmonium production as direct color singlet production with the appropriate quantum numbers. In the CSM, direct  $J/\psi$  and  $\psi'$  production required the emission of a hard gluon and should thus be rare on a perturbative timescale. However,  $\chi_c$ 's could be directly produced as color singlets and thus high  $p_T$   $J/\psi$  production should be dominated by  $\chi_c$  decays. The measurement of  $\chi_c$  relative to direct  $J/\psi$  production at the Tevatron collider [42] showed that the CSM was incomplete.

The non-relativistic QCD approach to quarkonium production was formulated [28] was formulated as a way to go beyond the CSM. NRQCD describes quarkonium production as an expansion in powers of  $v$ , the relative  $Q\bar{Q}$  velocity. Thus the angular momentum or color of the quarkonium state is not restricted to only the leading color singlet state but includes color octet production as well.

The  $x_F$  distribution of charmonium state  $C$  in NRQCD is

$$\frac{d\sigma_C}{dx_F} = \sum_{i,j} \sum_n \int_0^1 dx_1 dx_2 \delta(x_F - x_1 + x_2) f_i^p(x_1, \mu^2) f_j^A(x_2, \mu^2) C_{c\bar{c}[n]}^{ij} \langle \mathcal{O}_n^C \rangle, \quad (3)$$

where the partonic cross section is the product of perturbative expansion coefficients,  $C_{c\bar{c}[n]}^{ij}$ , and nonperturbative parameters describing the hadronization,  $\langle \mathcal{O}_n^C \rangle$ . We use the parameters determined by Beneke and Rothstein for fixed-target hadroproduction using the CTEQ 3L parton densities [43] with  $m_c = 1.5$  GeV and  $\mu = 2m_c$  [29]. Since the parameters  $\langle \mathcal{O}_n^C \rangle$  are fit to the LO calculation with a LO set of parton densities, no further  $K$  factor is required.

Direct  $J/\psi$  production has only contributions from  $g\bar{g}$  fusion and  $q\bar{q}$  annihilation [29], as in the CEM. The  $q\bar{q}$  contribution is all octet while the  $g\bar{g}$  component is a combination of octet and singlet production. The  $g\bar{g}$  partonic cross sections for  $J/\psi$  and  $\psi'$  production are

$$\hat{\sigma}(g\bar{g} \rightarrow \psi) = C_{c\bar{c}[n]}^{gg} \langle \mathcal{O}_n^\psi \rangle = B_8(x_1, x_2, s, m_c^2) \Delta_8(\psi) + B_1(x_1, x_2, s, m_c^2) \langle \mathcal{O}_1^\psi(^3S_1) \rangle \quad (4)$$

$\sqrt{s}$ (GeV)	Total $J/\psi$ (%)	Direct $J/\psi$ (%)	$\psi'$ (%)	$\sum_J \chi_{cJ} \rightarrow J/\psi$ (%)
17.3	66.6	90.7	75.2	8.9
29.1	62.6	86.7	66.2	6.3
41.6	60.4	84.7	61.9	5.0

Table 1: The percentage of charmonium production from color octets in NRQCD at each energy we consider.

where only the octet,  $\Delta_8^\psi = \langle \mathcal{O}_8^\psi(^1S_0) \rangle + (7/m_c^2) \langle \mathcal{O}_8^\psi(^3P_0) \rangle$ , and singlet,  $\langle \mathcal{O}_1^\psi(^3S_1) \rangle$ , matrix elements differ between  $J/\psi$  and  $\psi'$  production. The functions  $B_1$  and  $B_8$  are proportional to  $\alpha_s^2$  and  $\alpha_s^3$  respectively. The octet parameters are quite different for the two states:  $\Delta_8(J/\psi) \approx 5.8 \Delta_8(\psi')$ . The smaller  $\Delta_8(\psi')$  could be due to the larger mass and thus the increased “hardness” of the emitted gluon for the  $\psi'$ .

On the other hand, a color singlet  $\chi_c$  can be formed from two gluons [40, 41] so that  $\chi_c$  production is predominantly color singlet. In addition, the  $\chi_{c1}$  has a singlet contribution from  $gq$  scattering at  $\mathcal{O}(\alpha_s^3)$  [29]. Only the  $q\bar{q}$  channel contributes to color octet  $\chi_c$  production. Thus the largest singlet contribution to total  $J/\psi$  production is from  $\chi_{cJ}$  decays. Of these  $\chi_{cJ}$  decays, the most important is the  $\chi_{c1}$  which has a 27% branching ratio to  $J/\psi$ . The  $\chi_{c2}$  also has a relatively large branching ratio to  $J/\psi$ , 14%. Although the  $\chi_{c0}$  production cross section is as large as those of the other  $\chi_c$  states, its small branching ratio,  $< 1\%$ , results in a negligible  $\chi_{c0}$  contribution to  $J/\psi$  production. The  $\chi_{c0}$  is essentially invisible in hadroproduction experiments which reconstruct  $\chi_{cJ}$ ’s from their radiative decays to  $J/\psi$ .

The total  $J/\psi$   $x_F$  distribution then includes radiative decays of the three  $\chi_{cJ}$  states and hadronic decays of the  $\psi'$ ,

$$\frac{d\sigma_{J/\psi}}{dx_F} = \frac{d\sigma_{J/\psi}^{\text{dir}}}{dx_F} + \sum_{J=0}^2 B(\chi_{cJ} \rightarrow J/\psi X) \frac{d\sigma_{\chi_{cJ}}}{dx_F} + B(\psi' \rightarrow J/\psi X) \frac{d\sigma_{\psi'}}{dx_F}. \quad (5)$$

In Fig. 1 we show an example of the relative singlet and octet contributions to total  $J/\psi$ , direct  $J/\psi$ ,  $\psi'$  and the sum of the three  $\chi_c$  contributions to  $J/\psi$  production at 450 GeV, the SPS proton beam energy. Only the forward  $x_F$  distributions are shown since the distributions are symmetric around  $x_F = 0$ . No nuclear effects on the parton distribution functions are included.

The percentage octet production of each charmonium state is given in Table 1. The octet contribution decreases with energy for all charmonium states. Since color singlet  $\chi_{cJ}$  production is through the  $gg$  and  $gq$  channels, the fraction of octet  $\chi_{cJ}$  production is quite small, 10% or less. The decrease of octet production with energy is expected because the octet  $q\bar{q}$  contribution becomes even smaller at higher energies. On the other hand, direct  $J/\psi$  and  $\psi'$  production is color octet dominated since both the  $gg$  and  $q\bar{q}$  channels have octet contributions, see Eq. (4). The larger value of  $\Delta_8(J/\psi)$  relative to  $\Delta_8(\psi')$  increases the overall octet contribution from  $\sim 66\%$  for the  $\psi'$  to  $\sim 87\%$  for the direct  $J/\psi$  at  $\sqrt{s} = 29.1$  GeV. However, when the  $\chi_{cJ}$  radiative decays are included, the octet contribution to total  $J/\psi$  production is

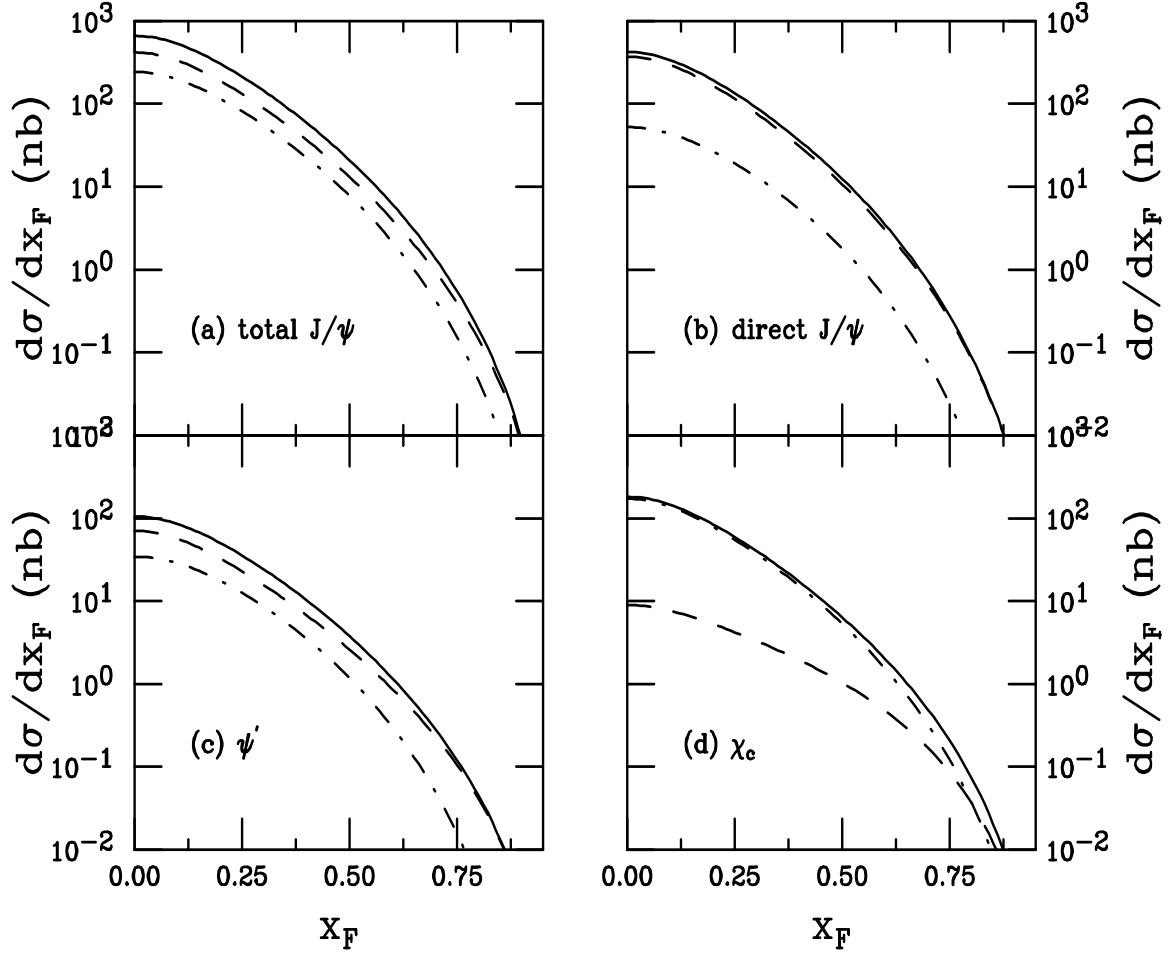


Figure 1: Charmonium  $x_F$  distributions at 450 GeV. The total  $J/\psi$  (a), direct  $J/\psi$  (b),  $\psi'$  (c) and summed  $\chi_{cJ}$  contributions to the  $J/\psi$  (d) cross sections are shown. The octet (dashed) and singlet (dot-dashed) contributions to the total (solid) are shown separately.

nearer to that of the  $\psi'$ ,  $\sim 63\%$ . These results are reflected in Fig. 1. Note also that the  $x_F$  distributions of the charmonium states are not exactly parallel to each other, as predicted by the CEM. Unfortunately the slopes of the  $x_F$  distributions are quite similar and it is not until relatively large values of  $x_F$  that the differences become more significant. However, there are other ways to distinguish the production mechanism since these two models of charmonium production lead to quite different predictions of the  $A$  dependence, as we will demonstrate in the next section.

### 3 Absorption by Nucleons

In Ref. [10], absorption was described in terms of the singlet and octet components of the  $J/\psi$  wavefunction,

$$|J/\psi\rangle = a_0|(c\bar{c})_1\rangle + a_1|(c\bar{c})_{8g}\rangle + a_2|(c\bar{c})_{1gg}\rangle + a'_2|(c\bar{c})_{8gg}\rangle + \dots \quad (6)$$

In the CSM [40, 41], only the first component is nonzero for direct  $J/\psi$  production. The  $c\bar{c}$  pairs then pass through nuclear matter in small color singlet states and reach their final state size outside the nucleus, at least when  $x_F > 0$ . If  $c\bar{c}$  pairs are predominantly produced in color octet states, then it is the  $|(c\bar{c})_{8g}\rangle$  state that interacts with nucleons. After the color octet  $c\bar{c}$  is produced, it can neutralize its color by a nonperturbative interaction with a gluon. This octet state is fragile so that a gluon exchanged between it and a nucleon would separate the  $(c\bar{c})_8$  from the gluon, exposing its color and, since the octet is unbound, break it up [10]. If the  $|(c\bar{c})_{8g}\rangle$  state is free to evolve without interaction, such as in  $pp$  collisions, the additional gluon would be absorbed by the octet  $c\bar{c}$  pair, hence ‘evaporating’ the color. The CEM does not then care about the relative coefficients in Eq. (6). As formulated in Ref. [29], the NRQCD model provides the leading coefficients in the expansion of the wavefunction in Eq. (6) and hence encompasses both singlet and octet production and absorption. In this section, we will describe the absorption of color singlets, color octets, and the combination of the two for final-state  $J/\psi$ ,  $\psi'$  and  $\chi_c$  production. Any differences in the  $A$  dependence of these states will be a consequence of this nucleon absorption. We calculate charmonium production in the CEM with pure octet and pure singlet absorption while NRQCD is used to determine the fraction of charmonium states production in color singlets and color octets. This then determines the rate of singlet and octet absorption in Eq. (6).

The effect of nuclear absorption alone on the  $J/\psi$  production cross section in  $pA$  collisions may be expressed as [44]

$$\sigma_{pA} = \sigma_{pN} \int d^2b \int_{-\infty}^{\infty} dz \rho_A(b, z) S^{\text{abs}}(b, z) \quad (7)$$

where  $b$  is the impact parameter and  $z$  is the longitudinal production point. When the production and absorption can be factorized, as in the CEM, and no other  $A$  dependent effects are included,  $\sigma_{pN}$  is independent of  $A$  and drops out of the calculation of  $\alpha$ . The nuclear absorption survival probability,  $S^{\text{abs}}$ , is

$$S^{\text{abs}}(b, z) = \exp \left\{ - \int_z^{\infty} dz' \rho_A(b, z') \sigma_{\text{abs}}(z' - z) \right\} \quad (8)$$

The nucleon absorption cross section,  $\sigma_{\text{abs}}$ , depends on where the state is produced and how far it travels through nuclear matter. Nuclear charge density distributions from data are used for  $\rho_A$  [45]. The effective  $A$  dependence is obtained from Eqs. (7) and (8) by integrating over  $z'$ ,  $z$ , and  $b$ . The full dependence on  $A$  can be related to  $\alpha(x_F)$  in Eq. (1) but  $\alpha$  is only constant if  $\sigma_{\text{abs}}$  is constant and independent of the production mechanism [30, 44]. The observed  $J/\psi$  yield includes an  $\approx 30\%$  contribution from  $\chi_{cJ}$  decays [33] and an  $\approx 12\%$  contribution from  $\psi'$  decays [27]. Then the total  $J/\psi$  survival probability is

$$S_{J/\psi}^{\text{abs}}(b, z) = 0.58 S_{J/\psi, \text{dir}}^{\text{abs}}(b, z) + 0.3 S_{\chi_{cJ}}^{\text{abs}}(b, z) + 0.12 S_{\psi'}^{\text{abs}}(b, z) . \quad (9)$$

The  $\psi'$  and  $\chi_c$  states are only produced directly since other, more massive, charmonium resonances lie above the  $D\bar{D}$  threshold and decay to  $D\bar{D}$  pairs.

We will present calculations for the total and direct  $J/\psi$ ,  $\psi'$ , and  $\chi_{cJ} \rightarrow J/\psi$   $A$  dependence. We include the  $\chi_{cJ}$  branching ratios to  $J/\psi$  because even though the  $\chi_{c0}$  cross section is large, the small branching ratio gives it a negligible contribution to the final-state  $J/\psi$  yield. Our results will be calculated at 158, 450, and 920 GeV, corresponding to the NA60 and HERA-B energies respectively. We calculate  $\alpha(x_F)$  for two targets in each experiment: Be and Pb for NA60; C and W for HERA-B.

### 3.1 CEM: color singlet absorption

We first discuss pure color singlet absorption. In this case,  $\sigma_{\text{abs}}$  depends on the size of the  $c\bar{c}$  pair as it traverses the nucleus. This was first described in terms of color transparency [46]. The  $c\bar{c}$  pairs are initially produced with a size on the order of its production time,  $r_{\text{init}} \sim \tau_{\text{init}} \propto m_c^{-1}$ . This initial size is ignored in the calculation. The charmonium formation time obtained from potential models [22] is  $\tau_C \sim 1 - 2$  fm, considerably longer. The absorption cross section of these small color singlet pairs grows as a function of proper time until  $\tau_C$  when it saturates at its asymptotic value  $\sigma_{CN}^s$  [30, 47, 48],

$$\sigma_{\text{abs}}(z' - z) = \begin{cases} \sigma_{CN}^s \left( \frac{\tau}{\tau_C} \right)^2 & \text{if } \tau < \tau_C \\ \sigma_{CN}^s & \text{otherwise} \end{cases} . \quad (10)$$

The proper time  $\tau$  is related to the path length through nuclear matter by  $\tau = (z' - z)/\gamma v$  where the  $\gamma$  factor introduces  $x_F$  and energy dependencies to  $\sigma_{\text{abs}}$ . At low energies and negative  $x_F$ , the  $c\bar{c}$  pair may hadronize inside a large nucleus.

Figure 2 illustrates the energy dependence of color singlet absorption in  $pA$  interactions. We take  $\sigma_{J/\psi N}^s = 2.5$  mb [49]. Assuming that the asymptotic absorption cross sections scale in proportion to the squares of the charmonium radii [50], we have  $\sigma_{\psi' N}^s \approx 3.7 \sigma_{J/\psi N}^s$  and  $\sigma_{\chi_{cJ} N}^s \approx 2.4 \sigma_{J/\psi N}^s$ . Thus each contribution to Eq. (9) has a different  $A$  dependence. The charmonium formation times are:  $\tau_{J/\psi} = 0.9$  fm,  $\tau_{\psi'} = 1.5$  fm, and  $\tau_{\chi_c} = 2.0$  fm [22]. The results at  $x_F < 0$  reflect the differences in formation times as well as the change in the  $\gamma$  factor due to their masses. The shorter formation time of the  $J/\psi$  allows it to reach its asymptotic size at large negative  $x_F$ .



At the lowest energy, 158 GeV, the charmonium states have a small chance of being formed inside the target at  $x_F > 0$  since  $\alpha \neq 1$  at  $x_F \sim 0.2$  although the deviation from unity is small. For higher energies, the charmonium states are produced outside the nucleus for  $x_F > 0$  so that  $\alpha \approx 1$ . No observable differences appear between the charmonium states at positive  $x_F$ . Indeed, this  $A$  dependence is in contradiction with all available data at  $x_F \approx 0$  unless other nuclear effects are included [30]. Therefore this picture of absorption is primarily useful for the interpretation of our calculations of pure octet absorption in the CEM and the combination of singlet and octet production and absorption in NRQCD.

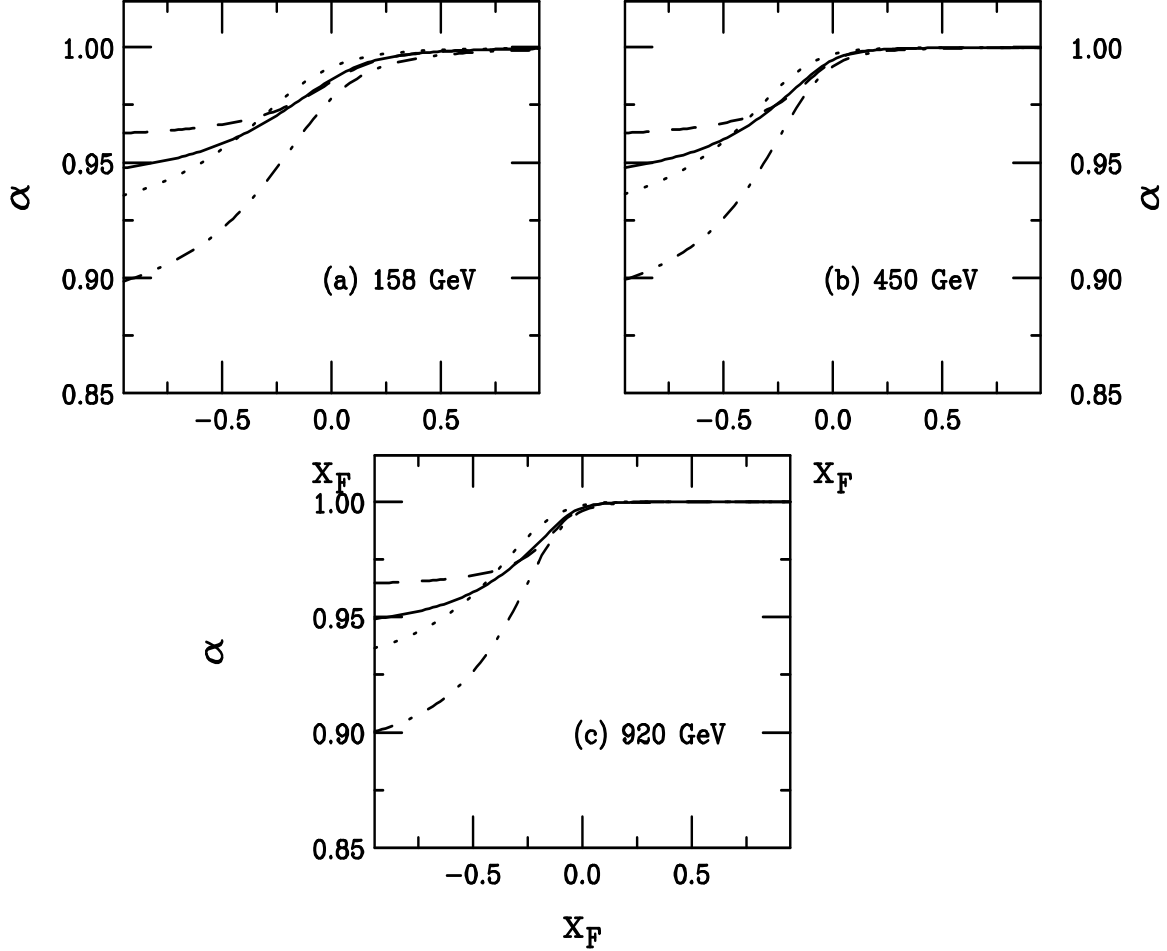


Figure 2: The  $A$  dependence for color singlet absorption is shown. The results are calculated at 158 GeV (a), 450 GeV (b), and 920 GeV (c). The total  $J/\psi$  (solid), the direct  $J/\psi$  (dashed), the  $\psi'$  (dot-dashed) and the  $\chi_c$  (dotted)  $A$  dependencies are given.

The direct  $J/\psi$   $A$  dependence (dashed curve) is weakest because its asymptotic cross section is smallest. The  $\psi'$   $A$  dependence (dot-dashed curve) is strongest because its final-state size and corresponding  $\sigma_{\text{abs}}$  is largest. In the calculation of Ref. [22], the  $\chi_c$  radius is somewhat smaller than that of the  $\psi'$  so that  $\sigma_{\psi'N}^s > \sigma_{\chi_c N}^s$ . The  $\chi_c$  formation time is the longest of the charmonium states and thus most likely to be

produced outside the target. Therefore the  $\chi_c$   $\alpha$  is actually slightly larger than that of the direct  $J/\psi$  at  $x_F \sim 0$  due to the longer  $\chi_c$  formation time (dotted curve). The  $\chi_c$  contribution to the  $A$  dependence of the total  $J/\psi$  yield (solid curve) decreases the total  $J/\psi$   $\alpha$  at large negative  $x_F$ , more like the  $\chi_c$ , while when  $x_F \rightarrow 0$ , the  $\chi_c$   $\alpha$  is near unity and the total and direct  $J/\psi$   $A$  dependencies are the same.

### 3.2 CEM: color octet absorption

On the other hand, if the  $c\bar{c}$  pairs are produced only in color octet states, they should hadronize after  $\tau_8 \sim 0.25$  fm in the  $c\bar{c}$  rest frame [49]. At large  $x_F$  in the lab frame, hadronization then occurs after the  $c\bar{c}$  has passed through the target as an octet. These fast  $c\bar{c}$  pairs thus remain color octets until after they have left the nucleus. However, at negative  $x_F$  it is possible for the octet states to neutralize their color inside the nucleus and interact as color singlets during the remainder of their path through the target [49]. This effect has typically been neglected when studying the  $A$  dependence of quarkonium production because the effect remains small in the  $x_F$  regions so far covered,  $x_F > -0.1$  [30, 44]. (See however Ref. [49].) While traveling through the nucleus as a pre-resonant  $|(c\bar{c})_{8g}\rangle$  state, the eventual identity of the final-state resonance is undetermined and all quarkonium states are absorbed with the same cross section,  $\sigma_{\text{abs}}^o$ . This physical picture agrees rather well with the empirical evidence that the  $J/\psi$  and  $\psi'$   $A$  dependencies are similar over the measured  $x_F$  range [5, 8]. We choose  $\sigma_{\text{abs}}^o = 3$  mb to agree with  $\alpha \approx 0.95$  for the  $J/\psi$  measured by the E866 collaboration at  $x_F = 0$  [8] when no other nuclear effects are considered. Note that this value is somewhat smaller than typically assumed for the color octet cross section [10] due to the relatively large measured  $\alpha$ .

We account for color neutralization of the octet in the nucleus in the following way: The path length of the  $|(c\bar{c})_{8g}\rangle$  through the nucleus is calculated in the nuclear rest frame. If it exceeds the maximum path length through the nucleus from the  $|(c\bar{c})_{8g}\rangle$  production point,  $\sigma_{\text{abs}}^o = 3$  mb for all charmonium states. This is the case for  $x_F \geq 0$  with all three energies. However, if color neutralization occurs before the state escapes the target, the resulting color singlet is absorbed according to Eq. (10).

The  $A$  dependence of color octet absorption is shown in Fig. 3. Note that at 158 GeV, color neutralization is achieved for  $x_F \leq -0.2$ . At higher energies, neutralization occurs in the target at larger negative  $x_F$ . It is important to remember that just because the octet color has been neutralized, the asymptotic cross section is not necessarily reached inside the target. With a formation time of less than 1 fm, only the  $J/\psi$  is likely to be fully formed in a large nucleus, as observed in the ‘saturation’ of the  $A$  dependence at  $x_F \leq -0.5$ . On the other hand, although the  $\psi'$  and  $\chi_c$  may become singlets inside the target, they do not reach their final-state size inside the target, even at  $x_F \rightarrow -1$ , due to the combination of their larger radii and longer formation times. The  $\psi'$  and  $\chi_c$   $A$  dependencies thus do not saturate, even at low energies. The slightly higher  $\alpha$  at 920 GeV is due to the different target  $A$  ratios chosen for the NA60 and HERA-B calculations, Pb/Be and W/C respectively.

We point out that the calculated  $\alpha$  is lower in the pure color octet picture at  $x_F \rightarrow -1$  than in the color singlet absorption model even though the same asymptotic

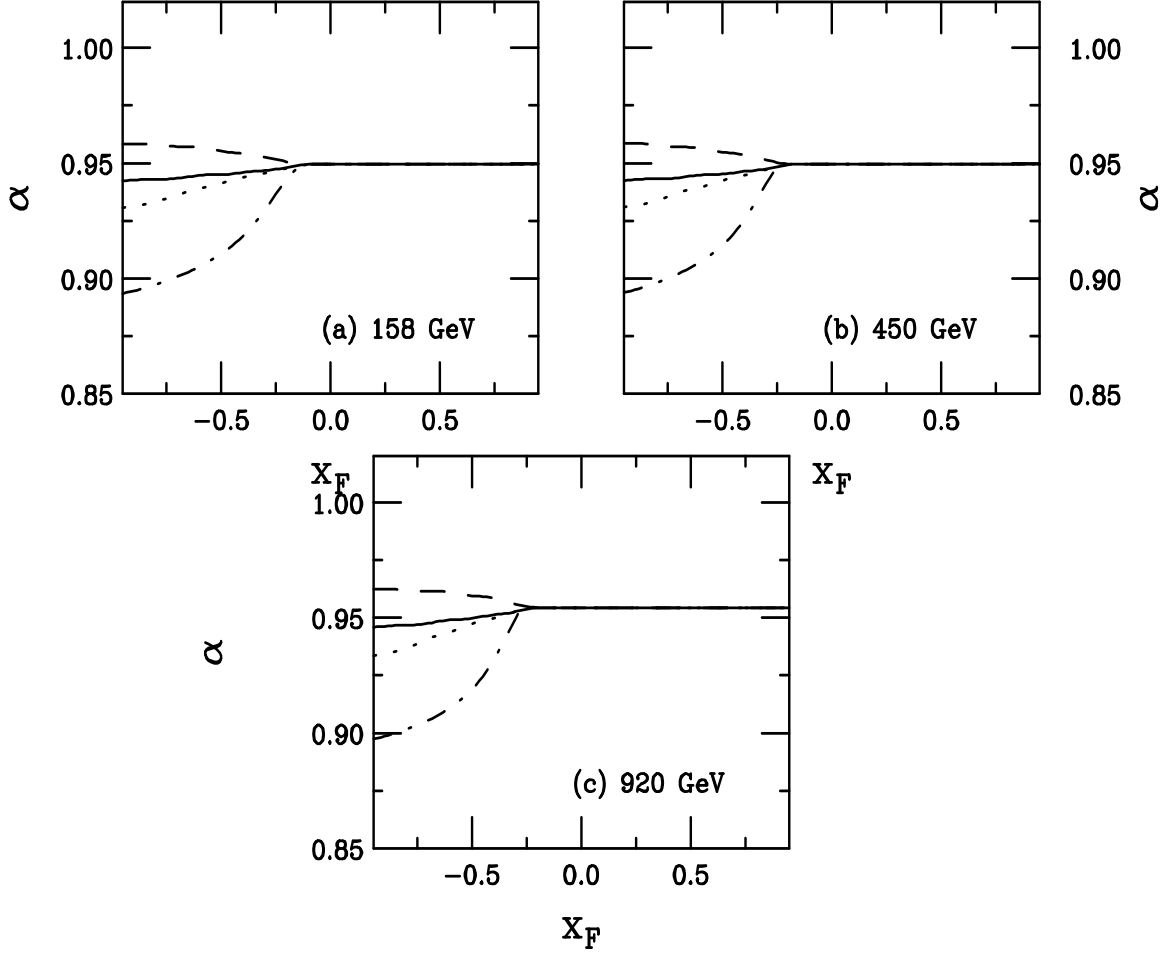


Figure 3: The  $A$  dependence for color octet absorption is shown. The results are calculated at 158 GeV (a), 450 GeV (b), and 920 GeV (c). The total  $J/\psi$  (solid), the direct  $J/\psi$  (dashed), the  $\psi'$  (dot-dashed) and the  $\chi_c$  (dotted)  $A$  dependencies are given.

color singlet cross sections are used. This is because now the state starts out as a color octet with a finite probability to be absorbed before neutralizing its color. The probability tends to be larger in real nuclei where the path length is calculated in the integral over impact parameter rather than in the empirical analytic model where an average path length is used [49]. The color octet is absorbed with its full cross section which is larger than the color singlet cross section at the point of absorption even though the asymptotic color singlet cross sections may be greater, *e.g.*  $\sigma_{\psi'N}^o < \sigma_{\psi'N}^s$ . The effective octet absorption cross section is larger because in the color octet state absorption has essentially no time delay.

The greatest differences in the  $A$  dependencies of the states are at intermediate to large negative  $x_F$  and would be most easily observable by NA60 at 158 GeV if their coverage extended so far. Note that, in this case also, the total  $J/\psi$  and the  $\chi_c$   $A$  dependencies would be quite similar in the target region while the  $\psi'$   $\alpha$  would be lower,  $\sim 0.9$  at 158 GeV and  $x_F = -0.5$  compared to  $\sim 0.93$  for the total  $J/\psi$

and  $\chi_c$ . However, only HERA-B has the capability to measure the  $A$  dependence at negative  $x_F$  and at the higher energy the differences appear at higher negative  $x_F$  and are generally not as large. Thus any distinction will be rather difficult to determine and the observed  $A$  dependence is likely to be the same within the experimental uncertainties for all charmonium states.

### 3.3 NRQCD: color singlet and color octet absorption

Recall that in the preceding discussion, only one type of  $c\bar{c}$  color state is assumed to be produced, either singlet or octet. Therefore the absorption factorizes from the production mechanism and the CEM cross section cancels in the calculation of  $\alpha$ , as in Eq. (7). The result is then independent of all parameters in the production process such as  $m_c$  and the parton densities. However, according to Eq. (6), charmonium production is through a combination of octet and singlet states. In this case, production and absorption are intimately related and the NRQCD cross section determines the relative octet proportion for each state as a function of  $x_F$  [51, 52]. The ratio of octet to singlet production is energy and  $x_F$  dependent, as shown in Table 1 and Fig. 1. Therefore Eq. (7) does not hold since  $\sigma_{pN}$  and  $S^{\text{abs}}$  do not factorize for all  $x_F$ .

We now give the unfactorized  $x_F$  distributions for each state in NRQCD. The  $x_F$  dependence of direct charmonium production and absorption is straightforward:

$$\frac{d\sigma_{pA}^{\psi}}{dx_F} = \int d^2b \left[ \frac{d\sigma_{pp}^{\psi, \text{oct}}}{dx_F} T_A^{\psi, \text{eff}(\text{oct})}(b) + \frac{d\sigma_{pp}^{\psi, \text{sing}}}{dx_F} T_A^{\psi, \text{eff}(\text{sing})}(b) \right], \quad (11)$$

$$\begin{aligned} \frac{d\sigma_{pA}^{\chi_{cJ} \rightarrow J/\psi X}}{dx_F} &= \int d^2b \sum_{J=0}^2 B(\chi_{cJ} \rightarrow J/\psi X) \left[ \frac{d\sigma_{pp}^{\chi_{cJ}, \text{oct}}}{dx_F} T_A^{\chi_{cJ}, \text{eff}(\text{oct})}(b) \right. \\ &\quad \left. + \frac{d\sigma_{pp}^{\chi_{cJ}, \text{sing}}}{dx_F} T_A^{\chi_{cJ}, \text{eff}(\text{sing})}(b) \right], \end{aligned} \quad (12)$$

where  $\psi = J/\psi$ ,  $\psi'$  and  $T_A^{\text{eff}} = \int dz \rho_A S^{\text{abs}}$  for both singlet and octet absorption. The  $pp$  subscript is used to denote unmodified parton distributions in the target. The total  $J/\psi$   $x_F$  distribution is more complex since it includes the feeddown from the  $\psi'$  and  $\chi_c$  states. Then [30]

$$\begin{aligned} \frac{d\sigma_{pA}^{J/\psi, \text{tot}}}{dx_F} &= \int d^2b \left\{ \left[ \frac{d\sigma_{pp}^{J/\psi, \text{dir, oct}}}{dx_F} T_A^{J/\psi, \text{eff}(\text{oct})}(b) \right. \right. \\ &\quad \left. \left. + \sum_{J=0}^2 B(\chi_{cJ} \rightarrow J/\psi X) \frac{d\sigma_{pp}^{\chi_{cJ}, \text{oct}}}{dx_F} T_A^{\chi_{cJ}, \text{eff}(\text{oct})}(b) + B(\psi' \rightarrow \psi X) \frac{d\sigma_{pp}^{\psi', \text{oct}}}{dx_F} T_A^{\chi_{cJ}, \text{eff}(\text{oct})}(b) \right] \right. \\ &\quad \left. + \left[ \frac{d\sigma_{pp}^{J/\psi, \text{dir, sing}}}{dx_F} T_A^{J/\psi, \text{dir, eff}(\text{sing})}(b) + \sum_{J=0}^2 B(\chi_{cJ} \rightarrow \psi X) \frac{d\sigma_{pp}^{\chi_{cJ}, \text{sing}}}{dx_F} T_A^{\chi_{cJ}, \text{eff}(\text{sing})}(b) \right. \right. \\ &\quad \left. \left. + B(\psi' \rightarrow \psi X) \frac{d\sigma_{pp}^{\psi', \text{sing}}}{dx_F} T_A^{\psi', \text{eff}(\text{sing})}(b) \right] \right\}. \end{aligned} \quad (13)$$

Our results are shown in Fig. 4. We have chosen the octet absorption cross section such that the total  $J/\psi$   $\alpha$  agrees in magnitude with the recent measurement by E866

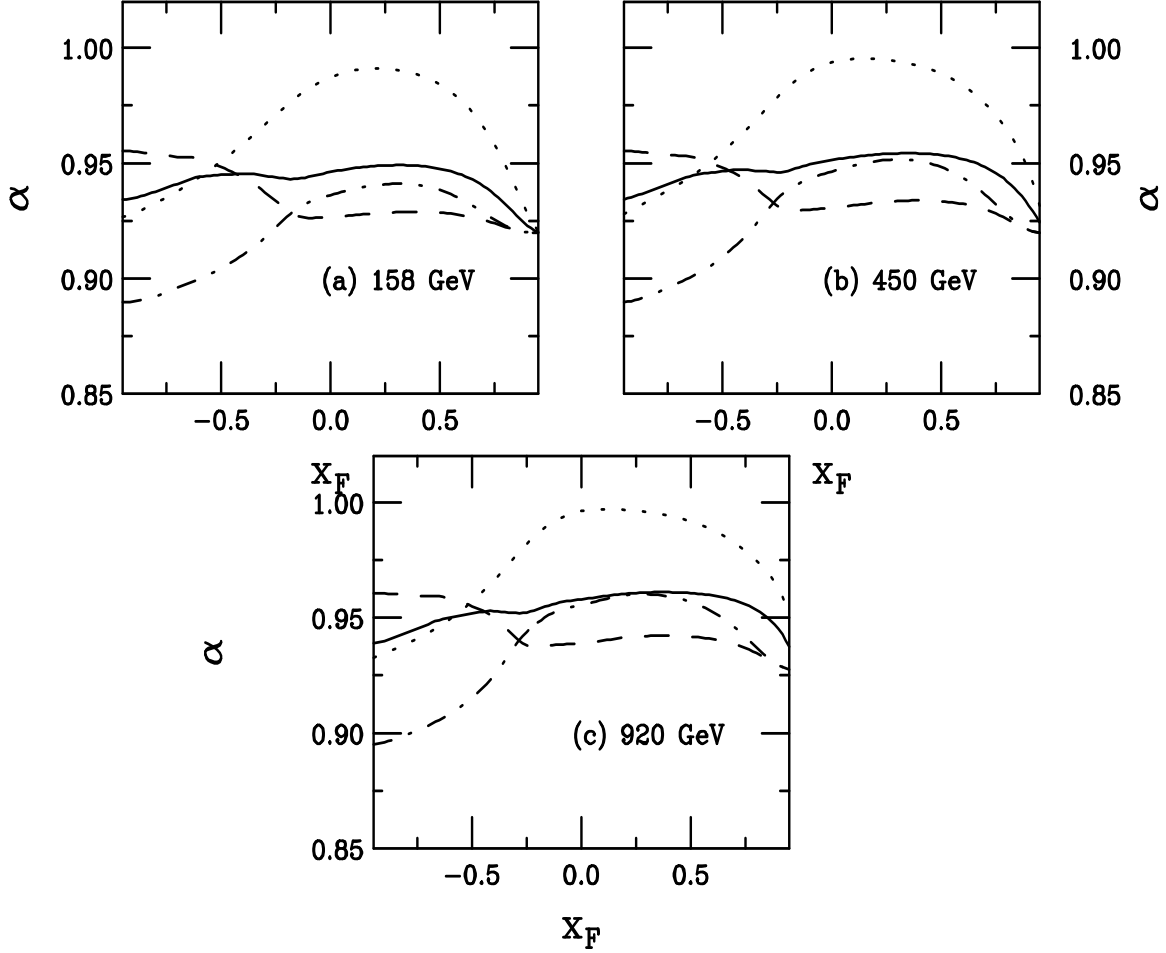


Figure 4: The  $A$  dependence for color singlet and color octet absorption in the NRQCD model is shown. The results are calculated at 158 GeV (a), 450 GeV (b), and 920 GeV (c). The total  $J/\psi$  (solid), the direct  $J/\psi$  (dashed), the  $\psi'$  (dot-dashed) and the  $\chi_c$  (dotted)  $A$  dependencies are given.

at 800 GeV [8]. In this case,  $\sigma_{J/\psi N}^{\text{oct}} = 5$  mb and  $\sigma_{J/\psi N}^{\text{sing}} = 2.5$  mb gives  $\alpha \approx 0.95$  at  $x_F \approx 0$ . The same octet cross section is then used for the octet component of the absorption for all charmonium states. If the octet state neutralizes its color, the resulting color singlet is absorbed according to Eq. (10). The same absorption cross sections are also used for the singlet component of charmonium production in section 3.1.

In Figs. 2 and 3, the predicted difference between  $J/\psi$ ,  $\psi'$  and  $\chi_c$  absorption was not large in the measurable region, particularly when the total  $J/\psi$   $A$  dependence was considered. Now, however, the  $\chi_c$  and total  $J/\psi$  results are significantly different and if the NRQCD model provides the right description of charmonium production, the measured  $\chi_c$   $A$  dependence should thus be quite different from that of the  $J/\psi$ . Note also that the  $\psi'$   $\alpha$  is slightly lower than the total  $J/\psi$   $\alpha$  at  $x_F \sim 0$ , in accordance with the E866 results [8].

The direct  $J/\psi$   $A$  dependence is rather similar to the octet results shown in Fig. 3

due to its large octet component. The  $\psi'$  has a larger overall singlet component but the singlet influence on the  $A$  dependence is rather weak. The main difference between direct  $J/\psi$  and  $\psi'$  production at  $x_F > 0$  is the larger  $\alpha$  of the  $\psi'$  due to the singlet component. However, the dominant color singlet component of  $\chi_c$  production leads to an almost linear  $A$  dependence for  $0 < x_F < 0.5$  at 158 GeV and  $-0.25 < x_F < 0.5$  at 920 GeV. The range of  $x_F$  at which  $\alpha \sim 1$  is broader at higher energies because the singlet  $gg$  contribution grows larger with energy. Given the similarities between the pure color singlet and color octet results at large negative  $x_F$ , it is difficult to disentangle the relative contributions for the combination of the two in this region. However, the differences at large positive  $x_F$  are due to the change in the relative octet/singlet contributions. At large  $x_F$ , the  $q\bar{q}$  component is more important. This octet piece causes the drop in  $\alpha$  of the  $\chi_c$  at large  $x_F$  while having little effect on the  $J/\psi$  and  $\psi'$ . Finally, we note that the total  $J/\psi$   $A$  dependence in this calculation is quite similar to the  $\psi'$  dependence, as already indicated by previous measurements [5, 8].

It is clear that if this model is correct, both NA60 and HERA-B should have no difficulty observing substantial differences in the  $J/\psi$  and  $\chi_c$   $A$  dependence since the values of  $\alpha$  are clearly different even at positive  $x_F$ . Other effects such as nuclear shadowing and energy loss would be similar for the two resonances so that differences in absorption mechanisms would not be washed out.

## 4 Conclusions

We have calculated the nuclear dependence of total and direct  $J/\psi$ ,  $\psi'$  and  $\chi_c$  due to absorption alone. We have studied absorption of pure color singlets and color octets in the context of the color evaporation model and a combination of octet and singlet production in nonrelativistic QCD. When considering charmonium production in a pure color state, as in the color evaporation model, we find little difference in the charmonium  $A$  dependencies in regions accessible to past experiments, in agreement with the  $J/\psi$  and  $\psi'$  measurements to date. However, when the  $\chi_c$  is considered, its large color singlet component results in a substantially different  $A$  dependence in the nonrelativistic QCD description. This difference should be easily detected by the two experiments that plan to measure  $\chi_c$  production, NA60 and HERA-B. Their results should quickly answer the question posed by the title of this paper.

**Acknowledgments** I would like to thank M. Bruinsma, D. Hansen, C. Lourenço, M. Medinnis, K. Redlich, H. Satz and A. Zoccoli for helpful discussions.

## References

- [1] J.C. Collins, D.E. Soper and G. Sterman, in *Perturbative Quantum Chromodynamics*, ed. A.H. Mueller (World Scientific, Singapore, 1989), p. 1.
- [2] D.M. Alde *et al.* (E772 Collab.), Phys. Rev. Lett. **66** (1991) 2479.

- [3] J. Badier *et al.* (NA3 Collab.), Z. Phys. **C20** (1983) 101.
- [4] S. Katsanevas *et al.*, Phys. Rev. Lett. **60** (1988) 2121.
- [5] D.M. Alde *et al.* (E772 Collab.), Phys. Rev. Lett. **66** (1991) 133.
- [6] M.J. Leitch *et al.* (E789 Collab.), Nucl. Phys. **A544** (1992) 197c.
- [7] M.C. Abreu *et al.* (NA50 Collab.), Phys. Lett. **B410** (1997) 327, 337.
- [8] M.J. Leitch (E866 Collab.), Phys. Rev. Lett. **84** (2000) 3256.
- [9] M.C. Abreu *et al.* (NA50 Collab.), Phys. Lett. **B477** (2000) 28.
- [10] D. Kharzeev and H. Satz, Phys. Lett. **B366** (1996) 316.
- [11] T.B.W. Kirk *et al.*, Phys. Rev. Lett. **42** (1979) 619.
- [12] C. Kourkouvelis *et al.*, Phys. Lett. **81B** (1979) 405.
- [13] A.G. Clark *et al.*, Nucl. Phys. **B142** (1978) 29.
- [14] S.R. Hahn *et al.*, Phys. Rev. **D30** (1984) 671.
- [15] D.A. Bauer *et al.*, Phys. Rev. Lett. **54** (1985) 753.
- [16] V. Koreshev *et al.*, Phys. Rev. Lett. **77** (1996) 429.
- [17] Y. Lemoigne *et al.*, Phys. Lett. **113B** (1982) 509.
- [18] L. Antoniazzi *et al.*, (E705 Collab.), Phys. Rev. **D46** (1992) 4828.
- [19] L. Antoniazzi *et al.*, (E705 Collab.), Phys. Rev. Lett. **70**, (1993) 383.
- [20] L. Antoniazzi *et al.*, (E705 Collab.), Phys. Rev. **D49** (1994) 543.
- [21] B. Ronceux *et al.*, (NA38 Collab.), Nucl. Phys. **A566** (1994) 371c.
- [22] F. Karsch, M.T. Mehr, and H. Satz, Z. Phys. **C37** (1988) 617.
- [23] A. Baldit *et al.* (NA60 Collab.), Proposal SPSC/P316, March 2000.
- [24] See <http://na60.web.cern.ch/NA60> for more details.
- [25] HERA-B Report on Status and Prospects, DESY-PRC 00/04.
- [26] M. Bruinsma, ‘Prospects for  $J/\psi$  Suppression Measurements at HERA-B’, poster presented at *Quark Matter* ’01, the 15<sup>th</sup> International Conference on Ultra-Relativistic Nucleus-Nucleus Collisions, Jan. 2001.
- [27] R.V. Gavai *et al.*, Int. J. Mod. Phys. **A10** (1995) 3043.
- [28] G.T. Bodwin, E. Braaten and G.P. Lepage, Phys. Rev. **D51** (1995) 1125.

- [29] M. Beneke and I.Z. Rothstein, Phys. Rev. **D54** (1996) 2005.
- [30] R. Vogt, Phys. Rev. **C61** (2000) 035203.
- [31] A.D. Martin, R.G. Roberts, and W.J. Stirling, and R.S. Thorne, Eur. Phys. J. **C4** (1998) 463.
- [32] A.D. Martin, R.G. Roberts, and W.J. Stirling, and R.S. Thorne, Phys. Lett. **B443** (1998) 301.
- [33] A. Sansoni (CDF Collab.), Nucl. Phys. **A510** (1996) 373c.
- [34] C. Lourenço *et al.* (NA38/NA50 Collab.), in Proceedings of EPS Int. Conf. on High Energy Physics, Brussels, Belgium, 1995, EPS HEP Conf. 1995:363, CERN-PRE-95-001.
- [35] V. Barger, W.Y. Keung, and R.N. Philips, Z. Phys. **C6** (1980) 169.
- [36] V. Barger, W.Y. Keung, and R.N. Philips, Phys. Lett. **91B** (1980) 253.
- [37] M.L. Mangano, P. Nason, and G. Ridolfi, Nucl. Phys. **B405** (1993) 507.
- [38] G.A. Schuler and R. Vogt, Phys. Lett. **B387** (1996) 181.
- [39] R. Vogt, Z. Phys. **C71** (1996) 475.
- [40] R. Baier and R. Rückl, Z. Phys. **C19** (1983) 251.
- [41] G.A. Schuler, hep-ph/9403387, CERN-TH.7170/94.
- [42] F. Abe *et al.* (CDF Collab.), Phys. Rev. Lett. **71** (1993) 3421.
- [43] H.L. Lai *et al.*, Phys. Rev. **D51** (1995) 4763.
- [44] R. Vogt, Phys. Rept. **310** (1999) 197.
- [45] C.W. deJager, H. deVries, and C. deVries, Atomic Data and Nuclear Data Tables **14** (1974) 485.
- [46] S.J. Brodsky and A.H. Mueller, Phys. Lett. **B206** (1988) 685.
- [47] S. Gavin and R. Vogt, Nucl. Phys. **B345** (1990) 104.
- [48] J.-P. Blaizot and J.-Y. Ollitrault, Phys. Lett. **217B** (1989) 386.
- [49] D. Kharzeev and H. Satz, Phys. Lett. **B356** (1995) 365.
- [50] J. Hüfner and B. Povh, Phys. Rev. Lett. **58** (1987) 1612.
- [51] X.-F. Zhang, C.-F. Qiao, X.-X. Yao, and W.-Q. Chao, hep-ph/9711237.



- [52] X.-F. Zhang, X.-X. Yao, W.-Q. Chao, and C.-F. Qiao, in proceedings of “Quarkonium Production in Relativistic Nuclear Collisions”, (Proceedings from the Institute for Nuclear Theory, Vol. 7), ed. X.-N. Wang and B. Jacak (World Scientific) p.111.